Chem Soc Rev

Fluorescent and Colorimetric Chemosensors for Pyrophosphate

Journal:	*Chemical Society Reviews*
Manuscript ID:	CS-TRV-10-2014-000353.R2
Article Type:	Tutorial Review
Date Submitted by the Author:	23-Oct-2014
Complete List of Authors:	Lee, Songyi; Ewha Womans University, Chemistry and Nano Science Yuen, Karen K. Y.; The University of Sydney, Chemistry Jolliffe, Katrina A; The University of Sydney, Chemistry Yoon, Juyoung; Ewha Womans University, Chemistry

Journal Name

RSCPublishing

ARTICLE

Fluorescent and Colorimetric Chemosensors for Pyrophosphate

Cite this: DOI: 10.1039/x0xx00000x

Songyi Lee,[a†] Karen K. Y. Yuen,[b†] Katrina A. Jolliffe[b*] and Juyoung Yoon[a*],

Received 00th January 2012,
Accepted 00th January 2012

DOI: 10.1039/x0xx00000x

www.rsc.org/

Pyrophosphate anions play key roles in various biological and chemical processes. During the last few years, many exciting results have emerged regarding the development of fluorescent and colorimetric sensors for this biologically important species. In this review, we will cover the fluorescent and colorimetric chemosensors developed for the detection of pyrophosphate (PPi) since 2010.

1. Introduction

The phosphate anion and its derivatives play fundamental roles in numerous biological and chemical processes. The ability to selectively recognize such anions in competitive solvents has potential applications across diverse fields including medicinal chemistry and diagnostics. This has led to vast interest in the development of selective receptors and sensors for anionic phosphate derivatives.[1-3] Pyrophosphate (PPi), the dimeric form of inorganic phosphate (Pi), which is a by-product of cellular hydrolysis of ATP, is a biologically important target given its role in many crucial reactions. The difference in pyrophosphate concentrations in a variety of biological environments could also be used to monitor or diagnose a number of diseases. For example, abnormally high levels of PPi in synovial fluid are observed for patients with calcium pyrophosphate dihydrate (CPPD) crystal deposition disease[4] while intracellular PPi levels have become an important indicator in cancer research.[5] In addition, the detection of pyrophosphate can be employed in real-time DNA sequencing. As such, the detection and imaging of PPi has become a highly important research target.

Compared to more conventional detection methods, fluorescent and colorimetric chemosensors are highly attractive approaches for sensing PPi. The fluorimetric approach is able to be rapidly performed, is highly sensitive, suitable for high-throughput screening applications, and most importantly can be used for real time bio-imaging, whereas colorimetric chemosensors can be used to sense PPi by employing common UV-vis absorption spectrometers and more impressively by naked-eye visualization. During the last few years, there have been many exciting results regarding the development of fluorescent and colorimetric chemosensors for this biologically important species. This review will cover the fluorescent and colorimetric chemosensors developed for the detection of pyrophosphate (PPi) since 2010. A general overview of the design and applications of chemosensors for PPi is provided in the first section. The latter sections describe sensors sub-categorized by different sensing mechanisms.

2. Strategies for the design of PPi chemosensors

The most common approaches to PPi chemosensors have adopted conventional hydrogen bonding interactions and/or charge interactions for directly binding to the anion. These binding sites are either covalently attached to a fluorescent or colorimetric tag, providing a direct response upon PPi binding, or alternatively may provide a binding site for a fluorescent or colorimetric indicator that can be used in an indicator displacement assay (IDA).

Common hydrogen bond donors include urea, thiourea, amide, pyrrole, imidazoliums, etc. However, even though most receptors contain multiple hydrogen bond donors that are carefully designed to provide a preorganized binding site for the PPi ion, the majority of receptors based solely on hydrogen bonding interactions display a significant drawback in that they are only capable of sensing PPi in pure organic solvent or in the presence of a small amount of water. However, the combination of these hydrogen bonding interactions with positively charged binding sites, such as ammonium, can alleviate this problem to some extent.

One of the most successful approaches so far for reversible binding of PPi is the utilization of interactions between metal ion binding sites and the phosphate group. In particular, the Zn^{2+}-dipicolylamine (DPA) group has proven to be a very effective binding motif for phosphate derivatives[6] and when two Zn^{2+}-DPA units are preorganized through an appropriate linker, selectivity for PPi over other phosphate derivatives is often induced.

Recently, an alternative approach to PPi sensing involving metal displacement has been identified as a simple and convenient technique. In this approach, a metal complex is

designed such that PPi has a stronger affinity for the metal ion than the ligand initially present, resulting in metal displacement upon PPi binding.

Besides these common binding approaches, a range of alternative small molecule based receptors, conjugated polymers, nanoparticles and quantum dots have been utilized to construct PPi chemosensors. In all of these systems, the PPi recognition event is signalled by mechanisms such as photo-induced electron transfer (PET), internal charge transfer (ICT) or excimer formation or by alternative mechanisms, e.g. aggregation enhanced fluorescence (AIE), all of which induce distinct fluorescent or colorimetric changes.

3. Pyrophosphate selective chemosensors

3.1. Hydrogen Bonding Interactions

Yoon and co-workers reported fluorescence sensing of PPi and Pi using the imidazolium anthracene derivative **1** (Fig. 1).[7] Among the various anions examined, selective fluorescence quenching effects and the appearance of excimer peaks at ~485 nm were observed only upon addition of PPi and Pi to **1**. Using fluorescence titrations in acetonitrile, the association constants of **1** with PPi and Pi were calculated as 6.19×10^6 M^{-1} and 4.68×10^5 M^{-1}, respectively. The efficient fluorescent quenching effects with PPi and Pi were attributed to a PET mechanism, in which strong $(C\text{-}H)^+ \ldots X^-$ type ionic hydrogen bonding interactions between the imidazolium moieties and phosphate groups play a key role. On the other hand, the new peaks observed at 485 nm correspond to the excimer peak of anthracene. These results also suggest that the bipyridine moiety in compound **1** acts as a template and an adequate linker to induce moderate selectivity for binding to PPi over Pi.[8]

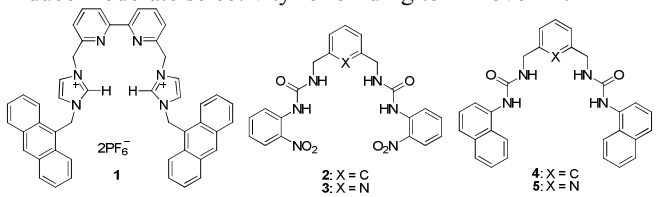

Fig. 1. Structures of the receptors **1**-**5**.

Bis-ureidic receptors **2**-**5** (Fig. 1) were synthesized by Caltagirone *et al*. Among PPi, Pi, $CH_3CO_2^-$, $C_6H_5CO_2^-$, glutarate and malonate ions, only PPi induced unique UV-vis absorption changes upon addition to compound **2**, such as disappearance of the band at 277 nm and the decrease of the band at 380 nm with a concomitant hypsochromic shift of 25 nm. These were attributed either to partial deprotonation or to an interaction with PPi *via* hydrogen bonding. Similar UV-vis absorption changes were observed for compound **3**. Clear naked eye colorimetric changes from yellow to red-orange were observed for both **2** and **3** upon the addition of 1 equiv. of PPi. Upon excitation at 345 nm, compound **4** displayed an emission band at 380 nm. When PPi was added, monomeric emission at 380 nm decreased and the excimer peak at 500 nm increased. Similar behaviour was also observed for compound **5**. Theoretical calculations indicated that, of the polyphosphates examined, only $HPpi^{3-}$ is capable of fitting into the pseudo-cavity of the receptor to induce excimer formation.

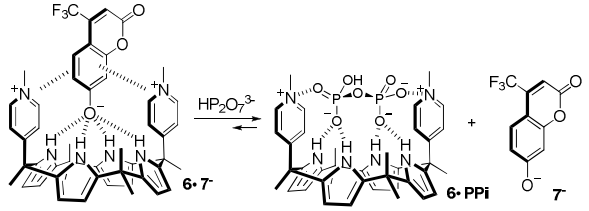

Fig. 2. Proposed displacement mechanism of chromenolate **7** from the bis-pyridinium calix[4]pyrrole derivative **6.**

A bis-pyridinium calix[4]pyrrole derivative **6** was reported as a unique receptor for PPi by Lee and co-workers (Fig. 2).[9] In this study, a complex of **6** with tetrabutylammonium-2-oxo-4-(trifluoromethyl)-2H-chromen-7-olate ($\mathbf{7}^-$) was used in an indicator displacement assay. The chromenolate anion ($\mathbf{7}^-$) forms a non-fluorescent complex with calix[4]pyrrole derivative **6**. Upon the addition of PPi, a selective fluorescence enhancement at 500 nm was observed as a result of the displaced chromenolate ion. Addition of F^- and Pi also resulted in a fluorescence enhancement, but to a much lower extent. In CH_3CN, the apparent association constant for this ensemble with PPi was calculated as $(2.55 \pm 0.12) \times 10^7$ M^{-1} with 1:1 stoichiometry. A similar "On-Off-On" fluorescence change for PPi was also observed in the presence of water. The apparent association constant of receptor **6** with PPi was reported as $(3.63 \pm 0.23) \times 10^6$ M^{-1} in 30% water. This value is 1/7 of that observed in pure CH_3CN. In contrast, in 30% water the apparent association constants for F^- and $H_2PO_4^-$ in CH_3CN were reduced to 1/276 and 1/140, respectively of those obtained in CH_3CN, which indicates that the selectivity for PPi over F^- and Pi improved dramatically in the presence of water. Electrostatic, anion-π and hydrogen bond interactions were reported as key factors for the selective recognition of PPi by **6**.

3.2. Chemosensors bearing Zn containing binding sites

He and co-workers utilized 1,2-diphenylethane-1,2-diamine as a unique template to synthesize the chiral dinuclear complexes **8**-$2Zn^{2+}$ and **8**-$2Cu^{2+}$ as chemosensors for PPi (Fig. 3).[10] In indicator displacement assays with pyrocatechol violet (PV), both **8**-$2Zn^{2+}$ and **8**-$2Cu^{2+}$ displayed a high selectivity for PPi over Pi, ATP, ADP, AMP, acetate and halogen anions in 10 mM HEPES buffer (pH 7.4). For the **8**-$2Zn^{2+}$-PV ensemble, addition of PPi resulted in a decrease of the absorption peak at 654 nm with a blue shift to 596 nm and an enhancement of the peak at 412 nm with a red shift to 442 nm, attributable to displacement of PV by PPi. These changes, which resulted in a colour change from dark blue to bright yellow, were readily observable by the naked eye. The apparent association constants of **8**-$2Zn^{2+}$ for PPi and Pi were determined to be $(7.9 \pm 0.9) \times 10^5$ M^{-1} and 284 M^{-1}, respectively while the association constant of **8**-$2Cu^{2+}$ for PPi was determined to be 862 M^{-1}. The binding phenomena of **8**-$2Zn^{2+}$ and **8**-$2Cu^{2+}$ could also be monitored by circular dichroism (CD) in the absence of PV.

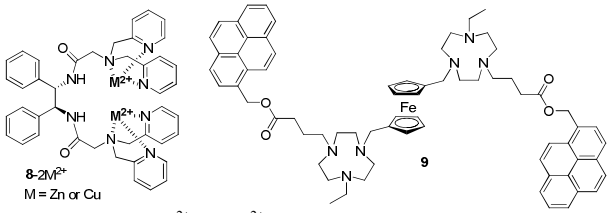

Fig. 3. Structures of **8**-2Zn^{2+}, **8**-2Cu^{2+} and **9**.

Spiccia and co-workers reported the **9**-2Zn^{2+} adduct (Fig. 3) as a selective fluorescent chemosensor for $P_2O_7^{4-}$ at pH 7.4 (CH_3CN-H_2O = 1:9, v/v).[11] The **9**-2Zn^{2+} complex showed monomer emission at 375 nm and weak excimer emission at 475 nm. The weak excimer emission was attributed to a favoured 'trans-like' configuration of the pyrene groups. When $P_2O_7^{4-}$ was added, excimer emission at 475 nm was enhanced 6-fold, which was attributed to the formation of a 1:1 **9**-2Zn^{2+}-PPi adduct resulting in the two pyrenes coming into close proximity. On the other hand, ATP and ADP induced relatively lower enhancement of the excimer emission and the addition of AMP, F^-, AcO^- and HPO_4^- did not induce any noticeable change in emission.

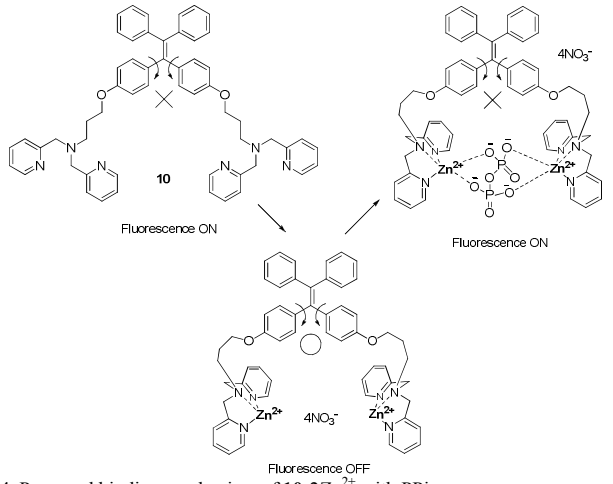

Fig. 4. Proposed binding mechanism of **10**-2Zn^{2+} with PPi.

The Hong group developed a tetraphenylethylene (TPE) derivative **10** bearing two Zn(II) DPA moieties as an aggregation-induced emission (AIE) fluorescent sensor for PPi.[12] In H_2O-DMSO (10:1, v/v), the addition of PPi induced 'turn-on' fluorescence emission due to the restriction of intramolecular rotation of the phenyl rings in **10**-2Zn^{2+}. The proposed mechanisms for binding and fluorescence changes are explained in Fig. 4. TPE derivative **10** showed strong emission at 472 nm due to enhanced AIE. On the other hand, the formation of **10**-2Zn^{2+} induces the destruction of aggregation, which results in decreased emission. Finally, the addition of PPi can revive the strong emission. The fluorescence intensity of **10**-2Zn^{2+} at 472 nm showed linear enhancement in the range of 0-60 μM PPi with a detection limit of 0.90 μM. Importantly, the fluorescence changes observed upon addition of AMP and ATP to **10**-2Zn^{2+} were relatively small compared to that of PPi and other simple anions did not induce any significant fluorescence change.

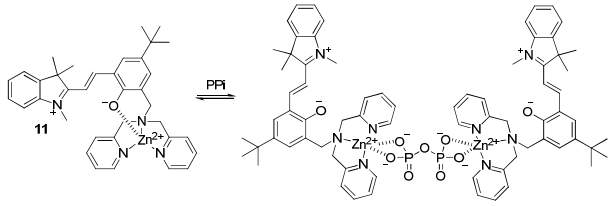

Fig. 5. Proposed binding mechanism of **11** with PPi.

Chan and co-workers reported a spiropyran based Zn^{2+}-DPA system **11** as a chemosensor for PPi.[13] In HEPES buffered ethanol (0.01 M, pH 7.4, 3:7 v/v), the addition of PPi to **11** resulted in enhanced fluorescence emission at 560 nm with a concomitant decrease at 620 nm providing a ratiometric change (Fig. 5). NMR studies indicated that the open merocyanine form of the ligand is present in the bound species. The stoichiometry between **11** and PPi was determined to be 2:1 with a log β of 8.6 and the detection limit of **11** for PPi was found to be 4×10^{-7} M. Common species in urine, such as K^+, Na^+, Ca^{2+}, Cl^-, SO_4^{2-}, $H_2PO_4^-$, urea, uric acid and bovine serum albumin (BSA) did not induce any significant change in fluorescence enabling the successful determination of PPi concentrations in urine samples using **11**.

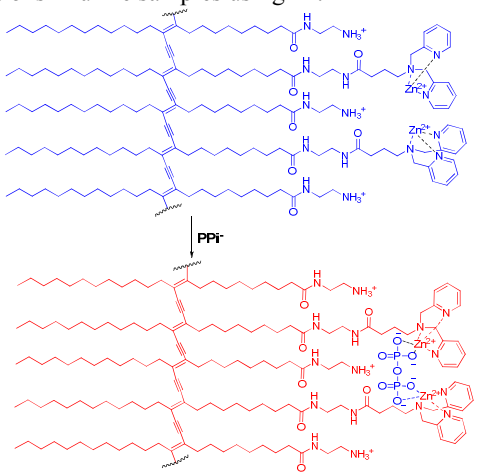

Fig. 6. Proposed mechanism for the PPi induced colorimetric change of Zn^{2+}-DPA PDAs.

Polydiacetylenes (PDAs) are known to undergo a unique colour change from blue to red upon environmental stimulation. A highly sensitive PDA for PPi was developed by Ahn and co-workers (Fig. 6).[14] A 1:1 mixture of two monomers, PCDA-EDA and PCDA-DEA-DPA, was self-assembled by sonication then cross-linked by UV irradiation followed by addition of Zn^{2+} to afford the Zn^{2+}-DPA PDA. Among various anions including N_3^-, AcO^-, CO_3^{2-}, Br^-, Cl^-, NO_3^-, SO_4^{2-}, ClO_4^-, $P_2O_7^{4-}$, and HPO_4^-, the Zn^{2+}-DPA PDAs showed selective colorimetric changes from blue to purple only for Pi and PPi at pH 7.0 (HEPES buffer). A microarray-chip assay system was also prepared using Zn^{2+}-DPA PDAs, in which the mixture of PCDA and PCDA-DEA-DPA (1:1) was immobilized onto a glass surface *via* a reaction of PCDA-EDA and glass coated in aldehyde groups. After the addition of Zn^{2+}, polymerization was induced by UV exposure to afford a liposome-microarray chip. PPi concentrations as low as 1 pM could be detected by this

liposome-microarray *via* fluorescent changes. The addition of PPi induced enhancement of red fluorescence, while addition of Pi did not result in any change. The enhanced selectivity for the chip array over the PDA in solution was attributed to the increased rigidity of the binding sites, where two Zn^{2+}-DPA units can provide a better binding site for PPi than Pi.

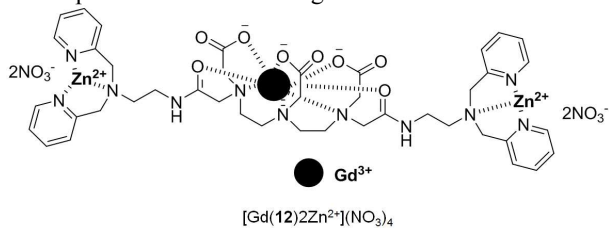

Fig. 7. Structure of [Gd(**12**)$2Zn^{2+}$]$(NO_3)_4$.

In an alternative approach to PPi recognition, Vilar and co-workers reported the relaxivity and colorimetric changes of functionalized lanthanide-DTPA-bis-amide complexes, [Gd(**12**)$2Zn^{2+}$]$(NO_3)_4$ (Fig. 7).[15] In indicator displacement assays with PV at pH 7.4 (10 mM HEPES), only the addition of PPi and ATP to the [Gd(**12**)$2Zn^{2+}$]$(NO_3)_4$-PV complex resulted in colorimetric changes from bright blue (bound PV) to yellow-brown (free PV). A number of other anions including Pi, phenyl phosphate, terephthalate, Fmoc-phosphotyrosine, Fmoc-phosphoserine, adenosine-5'-monophosphate (AMP) gave no response in this IDA, indicating the selectivity of the chemosensing ensemble for PPi and ATP. It was also demonstrated that PPi could modulate the relaxivity of [Gd(**12**)$2Zn^{2+}$]$(NO_3)_4$, which was large enough for imaging experiments. A stepwise binding process, with sequential formation of 1:1 then 1:2 complexes of [Gd(**12**)$2Zn^{2+}$]$(NO_3)_4$ with PPi, was proposed as a result of an inflexion of the relaxometric response after addition of 1 equiv. of PPi and this was confirmed by fluorescence titrations with the analogous europium complex.

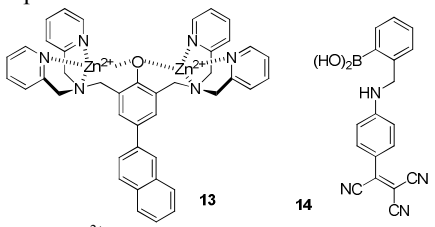

Fig. 8. Structures of bis Zn^{2+}-DPA complex **13** and boronic acid derivative **14**.

An ensemble composed of bis Zn^{2+}-DPA complex **13** and the boronic acid derivative **14** (Fig. 8) was reported as a fluorescent displacement assay for the selective and differential sensing of $P_2O_7^{4-}$ and nucleoside triphosphates.[16] At pH 10.5 (CAP buffer), Zn complex **13** showed an emission band at 440 nm, which was partially quenched upon addition of the boronic acid dye **14**. This partial fluorescence quenching was attributed to the interaction between the boronic acid in **14** and both Zn^{2+} sites in **13**. The addition of PPi to the ensemble **13**-**14** induced a remarkable 8-fold enhancement of emission intensity, as a result of the formation of the **13**-PPi complex with concomitant displacement of **14**. In contrast, addition of ATP, CTP, GTP and UTP to the **13**-**14** ensemble induced almost complete fluorescence quenching. This different fluorescence response with NTPs was attributed to the formation of ternary complexes **13**-**14**-**NTP** in which the two Zn^{2+} binding sites coordinated the phosphate moieties of the NTPs and the boronic acid moiety of **14** reacts with the OH groups of the sugar to form the corresponding boronate.

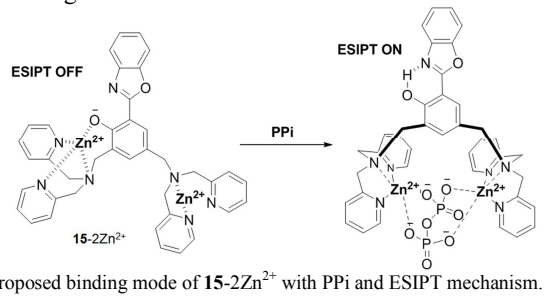

Fig. 9. Proposed binding mode of **15**-$2Zn^{2+}$ with PPi and ESIPT mechanism.

Pang and co-workers reported an excited state intramolecular proton transfer (ESIPT) based fluorescent probe for PPi. At pH 7.4 (10 mM HEPES), **15**-$2Zn^{2+}$ exhibits a selective and ratiometric fluorescence response to PPi over a range of other anions including ATP, HPO_4^{2-} and citrate, attributed to turn-on of the ESIPT.[17] **15**-$2Zn^{2+}$ displays an emission maximum at 420 nm, which undergoes a large bathochromic shift to 518 nm as a result of the *keto* emission arising from ESIPT as shown in Fig. 9. From fluorescence titrations, the association constant of **15**-$2Zn^{2+}$ with PPi was calculated to be 9.2×10^7 M^{-1}. **15**-$2Zn^{2+}$ was also capable of detecting PPi released from dNTPs in a PCR experiment.

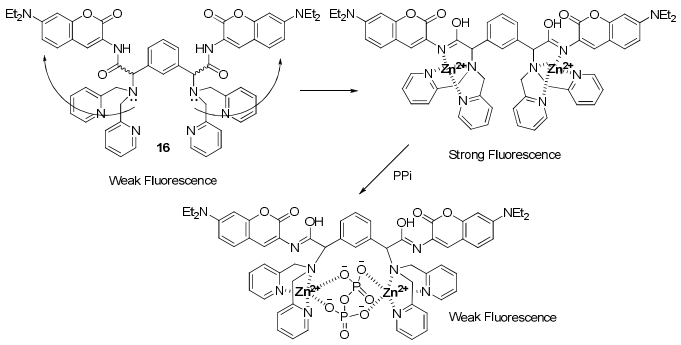

Fig. 10. Proposed mechanism for controlling the fluorescence of **16** by blocking and restoring PET.

Hong *et al.* reported a bis-coumarin derivative **16**-$2Zn^{2+}$ bearing two Zn-DPA binding sites as a fluorescent chemosensor for the detection of PPi in an aqueous HEPES buffer solution (10 mM, pH 7.4) (Fig. 10).[18] The addition of PPi to **16**-$2Zn^{2+}$ resulted in a fluorescence decrease by a factor of 9.8 and the detection limit for PPi was calculated to be 49 nM. Other anions examined, including ADP, AMP and Pi gave negligible changes in fluorescence. The proposed mechanisms for fluorescence changes observed on addition of PPi to **16**-$2Zn^{2+}$ are explained in Fig. 10. When Zn^{2+} was added to **16**, strong fluorescence emissions were turned on by blocking the photo-induced electron transfer (PET) process from the DPA amine. On the other hand, PPi binding would weaken the metal

coordination with the reductive quencher (the amine moiety), and induce fluorescence quenching by restoring the PET process.

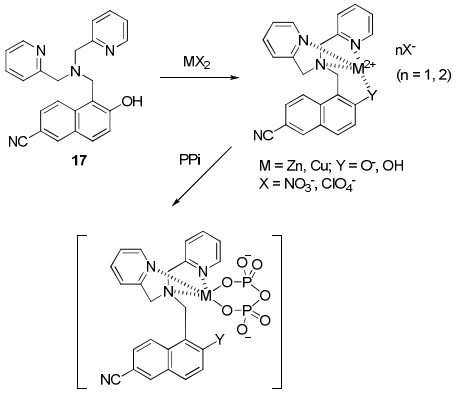

Fig. 11. Schematic presentation of the Zn(II) and Cu(II) complexes of DPA-hydroxynaphthalene **17**, and their PPi-bound complexes.

Mononuclear Zn^{2+}-DPA and Cu^{2+}-DPA complexes of 2-hydroxy-6-cyanonaphthalene derivatives have been reported to sense PPi selectively over ATP and other anions including Pi in HEPES buffer (10 mM, pH 7.4) (Fig. 11).[19] **17**-Cu^{2+} displayed highly selective turn-on fluorescence enhancement only for PPi among a variety of anions tested, including ATP, ADP, PO_4^{3-} and HPO_4^{2-}. **17**-Zn^{2+} also showed the largest fluorescence enhancement for PPi (~17-fold) with ATP inducing a relatively smaller increase and almost no change observed upon addition of other anions. From fluorescence titrations, the association constant for **17**-Zn^{2+} and PPi was reported as 1×10^5 M^{-1}. Interestingly, **17**-Zn^{2+} showed fluorescence enhancement in a time-dependent fashion, which was attributed to slow cleavage of the Zn-O bond as PPi binds to the Zn^{2+}.

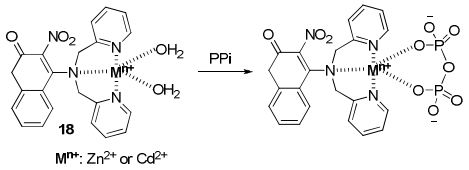

Fig. 12. Proposed binding mode of **18**-Zn^{2+} or **18**-Cd^{2+} with PPi.

Das and co-workers synthesized Zn^{2+} and Cd^{2+}-based complexes as selective fluorescent chemosensors for PPi (Fig. 12).[20] When Zn^{2+} was added to **18**, a selective "turn-on" fluorescence at 425 nm with a bathochromic shift of 31 nm was observed. A smaller enhancement with a bathochromic shift of 28 nm was observed on addition of Cd^{2+}. Among the various anions and nucleotides tested (including AMP, ADP, ATP and CTP) at pH 7.4 in HEPES buffer, **18**-Zn^{2+} and **18**-Cd^{2+} showed selective fluorescence changes only upon addition of PPi. A large fluorescence quenching effect was observed for **18**-Zn^{2+} upon the addition of PPi, while the addition of PPi induced moderate fluorescence enhancement for **18**-Cd^{2+}. The association constants of **18**-Zn^{2+} and **18**-Cd^{2+} towards PPi were calculated as 3.18×10^5 M^{-1} and 2.68×10^4 M^{-1}, respectively. Furthermore, **18**-Zn^{2+} and **18**-Cd^{2+} were successfully utilized to monitor the enzymatic activity of alkaline phosphatase (ALP).

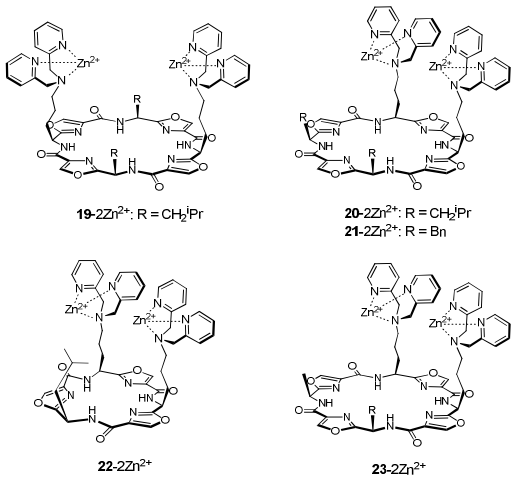

Fig. 13. Structures of dinuclear Zn(II) cyclic peptide-based anion receptors **19-2Zn^{2+}** - **23-2Zn^{2+}**.

Inspired by the *Lissoclinum* family of natural heterocycle-containing cyclic peptides, Jolliffe and co-workers have synthesized a family of macrocyclic peptides that possess two Zn^{2+}-DPA substituted side-arms and investigated their anion-binding properties using IDAs with either fluorescent or colorimetric indicators.[21-23] In order to gain better insight into the features required to achieve enhanced complementarity between the receptors and PPi, structural variants such as the spacing between the two Zn^{2+}-DPA binding moieties, the steric bulk and functionality of the 'non-binding' side chains, the size of the peptide scaffold and the distance between the scaffold and the Zn^{2+}-DPA binding sites were examined. Initial fluorescent IDAs with coumarin methylsulfonate as the indicator, it was observed that these receptors were selective for di- and tri-phosphate anions over monophosphates in a buffered aqueous environment (5 mM HEPES buffer, pH 7.4, 145 mM NaCl). In particular, improved discrimination between PPi, ATP and ADP was achieved when the Zn^{2+}-DPA pendant arms were brought into closer proximity (**20-2Zn^{2+}**–**21-2Zn^{2+}**); whilst selectivity was lost when the steric bulk of the non-binding side chains was increased (**19-2Zn^{2+}**, **22-2Zn^{2+}**).[21,22] Further experiments showed that selectivity for PPi over ATP and ADP was significantly enhanced in more competitive media (Kreb's saline buffer). Using colorimetric IDAs with PV and pyrogallol red it was found that naked-eye sensing of PPi was possible using these cyclic peptide derived chemosensing ensembles in the presence of more than 100 equiv. of ATP (**23-2Zn^{2+}**).[23]

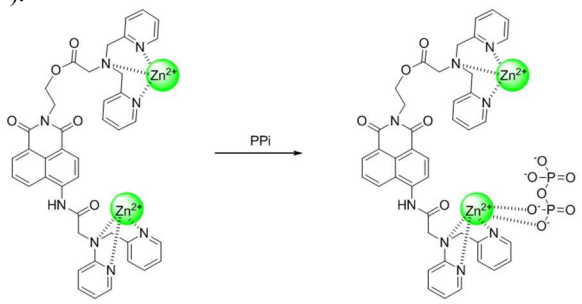

Fig. 14. Proposed binding mode of **24-2Zn^{2+}** with PPi.

Kim and co-workers reported a 1,8-naphthalimide-bis[Zn^{2+}-DPA] fluorescent chemosensor as a PPi-selective turn-off probe.[24] In buffered CH_3CN-HEPES solution [20 mM, pH 7.4, 5:95, v/v], **24–2Zn^{2+}** displayed significant fluorescence quenching upon binding to PPi (52%) and ATP (31%). Further examination of the fluorescence profiles revealed that binding to PPi also resulted in a large blue-shift (from 505 to 481 nm), whereas binding to ATP did not induce any notable change in emission wavelength. In contrast to most reported bis[Zn^{2+}-DPA] complexes, where binding to PPi usually involves both Zn^{2+} centres, molecular modelling suggests that only one Zn^{2+} centre of **24-2Zn^{2+}** interacts with PPi as shown in Fig. 14. The excellent selectivity of **24-2Zn^{2+}** towards PPi was exploited in cell imaging experiments, where **24-2Zn^{2+}** was successfully employed to show changes in intracellular (C2C12 cells) Zn^{2+} and PPi concentrations.

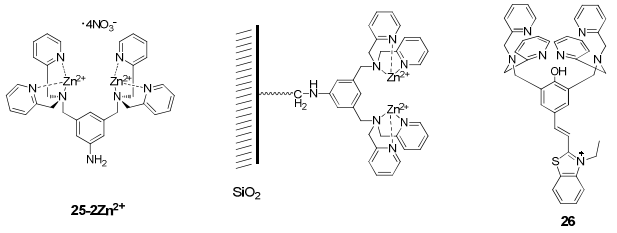

Fig. 15. Surface immobilization of PPi chelator **25-2Zn^{2+}** and structure of dual-mode probe **26**.

Liu and co-workers modified a previously established PPi recognition motif, containing two Zn^{2+}-DPA units on a *meta*-substituted xylyl scaffold, to enable the development of a surface immobilizable chelator for selective label-free electrical detection of PPi.[25] Chelator **25-2Zn^{2+}** was immobilized onto silicon-derived surfaces (coated with aldehyde group) *via* reduction amination to afford a Zn^{2+}-DPA-functionalized thin film (Fig. 15) and the surface properties and film thickness were characterized by ellipsometry, atomic force microscope (AFM) and surface–sensitive mass spectrometry (TOF-SIMS). Using a silicon-on-insulator field effect transistor (SOI–FET) device, Liu and co-workers investigated the PPi sensing ability of the new Zn^{2+}-DPA film. Upon exposure to 25 μM PPi in Tris buffer solution (pH 8), a signal response consistent with a field-effect caused by the binding of a positively charged molecule was observed. Despite the unexpected direction of the signal response, the authors were able to show through control experiments that the signal was indeed a result of complexation of PPi to the Zn^{2+}-DPA chelator.

Exploiting the advantages of using a near infrared (NIR) fluorophore, which include minimal overlap with autofluorescence from cells and favourable cell penetrating ability, Hong and co-workers synthesized a dual-mode fluorescent probe **26**, bearing a benzothiazolium hemicyanine chromophore and DPA binding moieties (Fig. 15).[26] The photophysical properties of **26-2Zn^{2+}** with PPi were evaluated and a bathochromic shift (27 nm) together with an increase in fluorescence intensity were observed upon the addition of PPi. However, ATP gave a similar, although slightly weaker, fluorescence response. A fluorescence titration gave an association constant of 4.4×10^7 M^{-1} for PPi. Despite the response to ATP, **26-2Zn^{2+}** was subsequently applied to *in vitro* fluorescence imaging of PPi using the C2C12 myoblast cell line, which revealed its potential in bioimaging experiments.

Fig. 16. A) Sensor **27-2Zn^{2+}**. B) Colour changes of sensor **27-2Zn^{2+}** in 50 mM aqueous HEPES buffer solution (pH 7.4), [**27-2Zn^{2+}**] = 35 μM, [other anions] = 175 μM. Anions from left to right: none, AMP, ADP, ATP, PO_4^{3-}, $H_2PO_4^-$, PhPi, NPhPi, PPi, F^-, Cl^-, Br^-, I^-, NO_3^-, SO_4^{2-}, HCO_3^-, $CH_3CO_2^-$, citrate, N_3^-, ClO_4^-, $S_2O_7^{2-}$, $C_2O_4^{2-}$.

The ease of performing naked eye visualization of anion binding, thus negating the need for instrumentation, renders colorimetric PPi sensors very attractive. With this in mind, Feng and co-workers developed a 7-nitrobenz-2-oxa-1,3-diazole(NBD)-phenoxo-bridged dinuclear Zn^{2+}-DPA colorimetric sensor that exhibits high selectivity for PPi in water (Fig. 16A).[27] Upon the addition of one equiv. of PPi, the aqueous buffered (50 mM, pH 7.4, HEPES) solution containing **27-2Zn^{2+}** showed an immediate colour change from red to purple as a result of a 25 nm red shift in the UV-vis absorbance band, from 501 to 526 nm. In contrast, only a slight colour change was observed when an excess of ATP was added and no colour changes were observed upon the addition of a range of other inorganic anions and organic phosphate anions (Fig. 16B). The apparent association constant between PPi and **27-2Zn^{2+}** was obtained *via* UV-vis titration and found to be approximately 3×10^8 M^{-1} in aqueous buffer, which is about 10000–fold, 4000–fold, 630–fold and 80-fold greater than those obtained for HPO_4^{2-}, AMP, ADP and ATP, respectively. Feng and co-workers further highlighted the superior selectivity of **27-2Zn^{2+}** by conducting similar UV-vis titrations in the presence of excess ATP, ADP or HPO_4^{2-}, where a significant colour change from red to purple was still observed upon the addition of PPi.

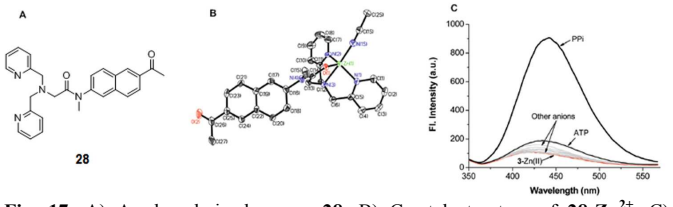

Fig. 17. A) Acedan derived sensor **28**. B) Crystal structure of **28-Zn^{2+}**. C) Fluorescence spectral change of **28-Zn^{2+}** upon addition of various anions (10 mM HEPES with 1% CH_3CN, pH 7.4) .

Given the drawbacks observed for many PPi probes which include low fluorescent enhancement, low sensitivity, slow response time and interference from nucleoside phosphates (ATP, ADP and AMP), Ahn *et al.* sought to address these

shortcomings with an acedan-based fluorescent mononuclear Zn^{2+}-DPA complex (Fig. 17).[28] The solid state structure of **28-Zn^{2+}** was characterised by single crystal x–ray crystallography, which revealed coordination between the oxygen of the carboxamido group and zinc (Fig. 17B). Upon addition of five equiv. of PPi to **28-Zn^{2+}**, a 10.1–fold fluorescence enhancement was observed, whereas the addition of other anions including F^-, Cl^-, OH^-, CN^-, CH_3COO^-, HSO_4^-, HPO_4^{2-}, PO_4^{3-}, AMP and ADP (five equiv. of each anion) resulted in negligible changes in fluorescence with the exception of ATP, which induced a small (1.86–fold) increase in fluorescence intensity (Fig. 17C). Ahn and co–workers attributed the fluorescence enhancement to binding induced breaking or weakening of the metal coordination by the carboxamido group, which in turn increases intramolecular charge transfer in the acedan moiety.

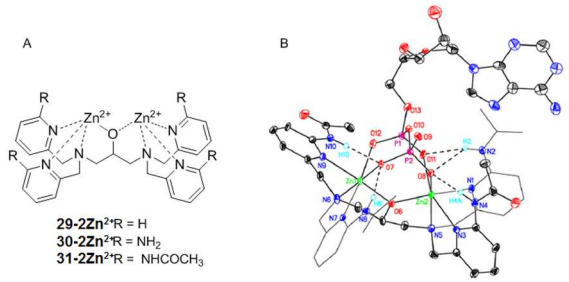

Fig. 18. A) Structures of complexes **29-2Zn^{2+} - 31-2Zn^{2+}**. B) Crystal structure of **31-2Zn^{2+}-ADP** complex.

Feng and co–workers introduced hydrogen bond donors onto their Zn^{2+}-DPA receptors in order to improve both binding affinity and selectivity for PPi in an aqueous environment.[29] To gauge the degree of improvement in the binding affinities and selectivities they also synthesised **29-2Zn^{2+}** as a control (Fig. 18A). Using an indicator displacement assay (IDA) with PV, it was found that **29-2Zn^{2+}** demonstrated high selectivity for PPi over a range of other anions, which included halides, nitrate, sulfate and inorganic phosphate. However, **29-2Zn^{2+}** was not capable of discriminating between citrate and PPi using this IDA, with a similar colour change observed for both anions. In contrast, an IDA with **30-2Zn^{2+}**, which incorporates NH_2 groups into the binding ligands, was found to show selectivity for PPi over other anions, including citrate. This improvement in binding selectivity led to the synthesis of **31-2Zn^{2+}**, which possesses four carboxyamido groups. With carboxyamido groups being better hydrogen bond donors than the aminopyridyl groups, it was anticipated that **31-2Zn^{2+}** would display better binding affinity and higher selectivity for PPi. The association constant between PPi and **31-2Zn^{2+}** was determined by competitive UV-vis titration to be $(1.2 \pm 0.2) \times 10^8$ M^{-1}, which is approximately 4-fold and 1000-fold greater than those of **30-2Zn^{2+}** and **29-2Zn^{2+}**, respectively. Analysis of the crystal structure of **31-2Zn^{2+}-ADP** indicated that the observed improvements in binding affinity were a result of the synergistic interaction between metal-ligand coordination and hydrogen–bonding analogous to that seen in metalloenzymes (Fig. 18B).

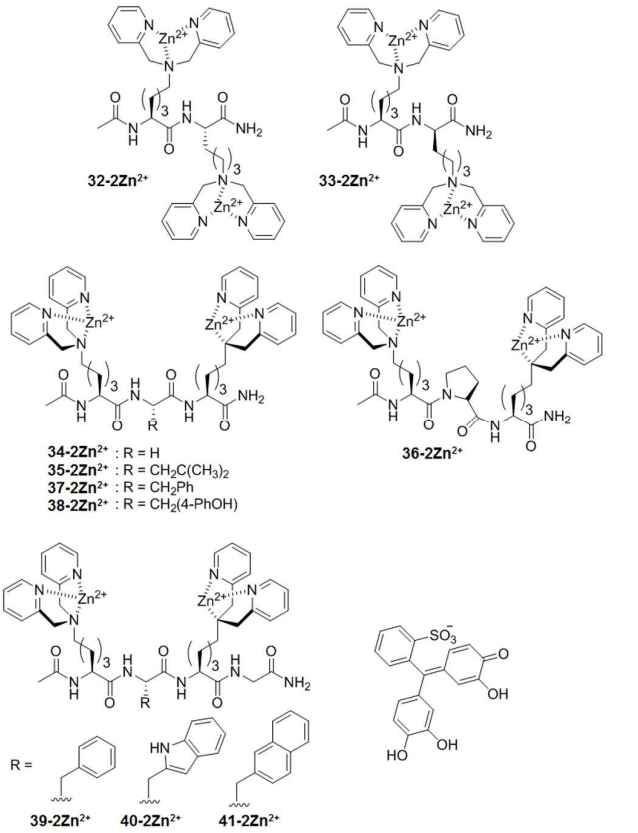

Fig. 19. Structures of linear peptide-based DPA receptors **32-2Zn^{2+} - 41-2Zn^{2+}** and the indicator, pyrocatechol violet.

Having already described a number of cyclic peptide derivatives bearing Zn^{2+}-DPA functionalized side chains for PPi recognition, the Jolliffe group applied their concept to simpler linear peptides, which can be readily obtained by solid phase synthesis.[30] Bis[Zn^{2+}-DPA] complexes **32-41**-2Zn^{2+} were used in colorimetric indicator displacement assays (IDAs) with pyrocatechol violet (Fig. 19), to enable rapid screening of their anion binding affinities by naked–eye detection, which was then confirmed by UV-vis spectroscopy. At pH 7.4 (5 mM HEPES, 145 mM NaCl), a variety of analytes including PPi, Pi, ATP, ADP, AMP, cAMP, pThr, pSer, citrate, SO_4^{2-} and HPO_4^{2-} were evaluated, but only PPi, ATP and ADP induced colorimetric changes in most cases. In addition, selectivities for PPi (log K_a ranging from 7.8 to 9) over ATP and ADP were observed for most of these systems. In particular, the Zn^{2+} complexes of **33**, **40** and **41** displayed strong binding affinities for PPi with good selectivity over ATP and ADP. Dipeptide receptor **33**-2Zn^{2+} bearing alternating L- and D-amino acids exhibited excellent selectivity for PPi over ATP and ADP, which indicates that positioning two Zn^{2+}-DPA side chains on the same face of the scaffold can be used to enhance selectivity.

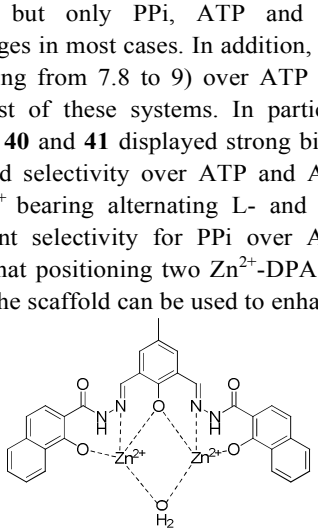

Fig. 20. Structure of **42-2Zn^{2+}** complex.

Mukherjee and co–workers reported the synthesis of the naphthalene carbohydrazone based dinuclear Zn(II) chemosensor **42-2Zn^{2+}**, together with its anion binding properties as determined using both fluorescence and UV-vis studies (Fig. 20).[31] Upon addition of various anions including F^-, Cl^-, Br^-, I^-, CH_3COO^-, HCO_3^-, NO_2^-, SO_4^{2-}, PO_4^{3-}, ADP and ATP, only the addition of PPi resulted in changes in the absorption spectrum of **42-2Zn^{2+}**. Similarly only addition of PPi resulted in changes in the fluorescence profile, where the emission band was shifted to a longer wavelength together with a dramatic fluorescence enhancement. Both fluorescence and UV-vis studies indicated that **42-2Zn^{2+}** is highly selective for PPi over other anions. Furthermore, Mukherjee and co-workers also demonstrated that **42-2Zn^{2+}** has a low PPi detection limit of 1.55×10^{-9} M *via* competitive fluorescence titrations and this characteristic was subsequently exploited in the monitoring of a polymerase-chain-reaction (PCR).

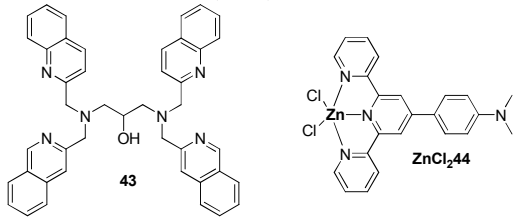

Fig. 21. Structures of **43** and **ZnCl$_2$44**.

Konno *et al.* reported the quinoline-based dinuclear Zn(II) complex **43-2Zn^{2+}** as a fluorescent sensor for PPi (Fig. 21).[32] In the absence of PPi, complex **43–2Zn^{2+}** displayed only weak fluorescence, but an 8-fold fluorescence enhancement was observed upon the addition of 1 equiv. of PPi. However, with the addition of more PPi (15 equiv.), fluorescence was quenched completely. Both UV-vis spectra and electrospray ionization mass spectrometry measurements indicated that this quenching was a result of the decomplexation of **43-2Zn^{2+}** in the presence of excess PPi. It was also noted that the anion–induced fluorescence enhancement was specific to PPi as this response was observed only to a small extent for ATP and ADP and not at all for other anions. To further probe the fluorescence response towards PPi, Konno and co-workers carried out a crystallographic investigation using diphenyl pyrophosphate (Ph_2PPi) as a crystallisable substitute for PPi. This allowed the authors to attribute the unique fluorescence response to the formation of an intramolecular excimer of the two quinoline groups as they come into close proximity upon Ph_2PPi binding.

Rissanen and co-workers recently reported the terpyridine-Zn^{2+} complex (**ZnCl$_2$44**) as a highly selective fluorescent sensor for PPi at pH 7.4 (10 mM HEPES buffer) (Fig. 21).[33] An approximately 500-fold enhancement of fluorescence at 591 nm was observed upon the addition of 1 equiv. of PPi to a 50 μM solution of **ZnCl$_2$44**. A detectable fluorescent response could be observed at PPi concentrations as low as 20 nM and the lowest limit of detection (LOD) was reported to be 0.8 nM. The **ZnCl$_2$44** complex was also successfully used to image PPi in HeLa cells, giving a bright orange-yellow emission. Moreover, **ZnCl$_2$44** formed a unique self–assembled hydrogel, which consists of a fibrous structure with fibre dimensions of 50 to 120 nm. This hydrogel was used to make gel coated paper strips, which show bright orange emission upon drop-casting with PPi.

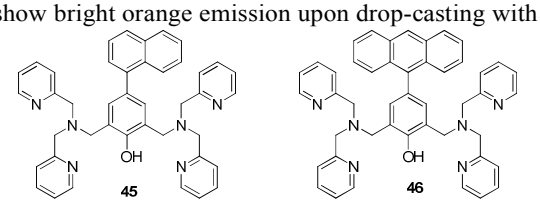

Fig. 22. Structures of 1-naphthyl and 9-anthracenyl analogues, **45** and **46**.

Tuck *et al.* developed a facile two-step synthesis of the bis-Zn(II)DPA fluorescent PPi sensors **45-2Zn^{2+}** and **46-2Zn^{2+}** (Fig. 22).[34] Upon addition of various biologically significant anions including AMP, Cl^-, Pi, $CH_3CO_2^-$ and HCO_3^-, **45-2Zn^{2+}** exhibited negligible changes in fluorescence emission, with the addition of GTP, ADP and ATP resulting in a minimal increase in fluorescence as compared to addition of PPi, for which emission was dramatically enhanced (7-fold increase upon addition of 1 equiv. of PPi), accompanied by a bathochromic shift from 450 nm to 464 nm. The apparent association constant of **45-2Zn^{2+}** for PPi was determined to be 7.2×10^5 M^{-1}. In contrast, the fluorescence of **46-2Zn^{2+}** was quenched completely upon complexation to PPi (3 equiv.), with a bathochromic shift of 38 nm. Moreover, additions of other anions such as AMP, Cl^-, $CH_3CO_2^-$ and HCO_3^- caused minimal to negligible decrease in fluorescence, whilst the addition of ADP and ATP resulted in significant quenching and smaller bathochromic shifts. The apparent association constant of **47-2Zn^{2+}** for PPi was estimated to be 1.2×10^6 M^{-1}. Tuck *et al.* also demonstrated the utility of these chemosensors by successfully monitoring both production and consumption of PPi during enzyme catalysed reactions.

3.3. Chemosensors bearing other metal containing binding sites

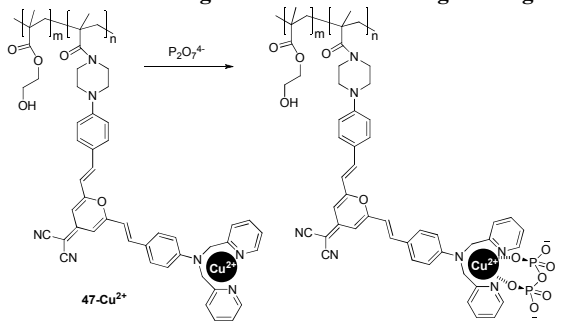

Fig. 23. Proposed mechanism of the recognition of PPi using copolymer **47**.

Tian and co-workers prepared hydrophilic copolymer **47** containing dicyanomethylene-4H-pyran groups as fluorescent communicating groups together with DPA units to bind Cu^{2+}, for the selective recognition of PPi in aqueous solution (Fig. 23).[35] At pH 7.4 in CH_3CH_2OH:H_2O (5:2, v/v), copolymer **47** displayed fluorescence emission at 605 nm (λ_{ex} = 460 nm). When Cu^{2+} was added to this solution, the fluorescence emission at 605 nm was almost completely quenched, which

was attributed to complex formation decreasing the intramolecular charge transfer (ICT) process from the DPA donor. Among various anions such as F^-, Cl^-, Br^-, I^-, $H_2PO_4^-$, HCO_3^-, HSO_4^-, AcO^-, NO_3^-, HPO_4^{2-}, SO_4^{2-}, CO_3^{2-}, AMP, ADP, ATP, PO_4^{3-}, only PPi induced a selective fluorescence enhancement by a factor of 4.8-fold. This was attributed to the interactions between PPi and **47**-Cu^{2+} reducing the binding interaction between Cu^{2+} and the DPA unit resulting in an enhancement of the electron-donating character of the amino groups and turn-on of the ICT. A thin film of **47**-Cu^{2+} on quartz slides also displayed a similar "turn-on" fluorescence.

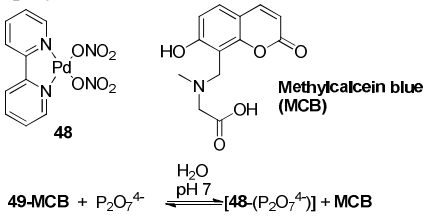

Fig. 24. Complexation of PPi to the Pd complex **48.**

In an alternative approach to PPi sensing, Severin and co-workers reported a PPi selective chemosensing ensemble **49-MCB**, incorporating the Pd complex **48** [$Pd(NO_3)_2$(bipy)] and a fluorescent dye (MCB = methylcalcein blue) (Fig. 24).[36] The addition of PPi to this ensemble in aqueous solution (HEPES at pH 7) resulted in a strong turn-on fluorescence signal at 440 nm attributable to the displaced MCB. A dynamic range of approximately 50-450 μM and a detection limit of 50 μM were reported for PPi. This sensing ensemble displayed high selectivity for PPi over other anions, such as F^-, Cl^-, Br^-, $H_2PO_4^-$, ClO_4^-, SO_4^{2-}, AcO^-, HCO_3^-, NO_3^- and salicylate.

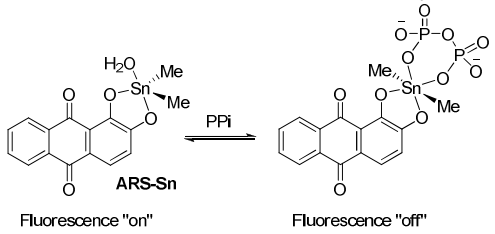

Fig. 25. Proposed binding mode of **ARS−Sn** with PPi.

Yatsimirsky and coworker reported the first example of an alizarin red S (ARS)-dimethyltin complex as an optical anion sensor for PPi at pH 6.7 in 5 mM phosphate buffer solution.[37] Addition of Me_2SnCl_2 to ARS to form ARS-Sn was found to induce a 100-fold fluorescence enhancement at 610 nm and the association constant of ARS with Me_2SnCl_2 was calculated as $(6.3 \pm 0.3) \times 10^4$ M^{-1} with 1:1 stoichiometry. Addition of PPi to the chemosensing ensemble resulted in almost complete fluorescence quenching, attributed to the initial formation of a ternary complex (Fig. 25). In contrast, addition of ATP and ADP induced 30% and 20% quenching, respectively, whereas addition of monophosphate species gave little response. From titration experiments, association constants for PPi and ATP with ARS-Sn were determined to be $(5.9 \pm 0.3) \times 10^4$ and 920 ± 80 M^{-1}, respectively and the detection limit for PPi was calculated as 3 μM with the linear range to 40 μM. The incomplete fluorescence quenching observed upon addition of ATP and ADP is suggested to be a result of weaker binding of these less basic anions to the ARS-Sn complex.

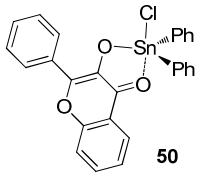

Fig. 26. Structure of complex **50**.

In an extension of this work, the Yatsimirsky group employed 3-hydroxyflavonate(Ofl)-diphenyltin(IV) chloride (Ph_2Sn(Ofl)Cl) as a selective fluorescent chemosensor for PPi.[38] Complex **50** (Fig. 26) showed strong fluorescence in non–aqueous media but a significant decrease in fluorescence was observed in the presence of water above 10% vol. However, the strong fluorescence at 646 nm observed upon excitation at 400 nm could be maintained in neutral aqueous solutions containing 5 mM cetyltrimethylammonium chloride. The addition of PPi to **50** induced selective fluorescence quenching due to the formation of $(Ph_2Sn(Ofl))_3PPi$, which was further converted to Ph_2Sn(Ofl)(PPi) in the presence of higher concentrations of PPi. Importantly, this system can sense PPi (1 μM) in the presence of a 100–fold excess of Pi, AMP, ADP and acetate, and even a 10–fold excess of ATP. The detection limit for PPi was calculated as 0.1 μM with a linear range of 0−5 μM.

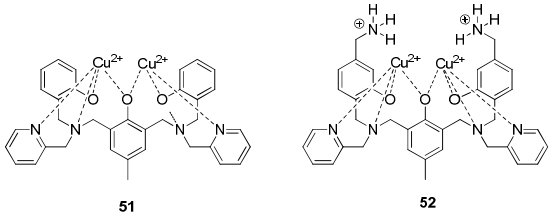

Fig. 27. Structures of Cu^{2+} complexes **51** and **52**.

Chen and co-workers have reported Cu^{2+}-containing DPA receptors **51** and **52**, which differ in the absence or presence of additional ammonium binding moieties, respectively for the colorimetric sensing of PPi using an IDA with PV (Fig. 27).[39] In HEPES buffer solution (10 mM, pH 7.0), both receptors bind to PV with 1:1 stoichiometry (as determined by Job's plot), with association constants for PV of 3.54×10^5 M^{-1} and 1.90×10^7 M^{-1}, respectively indicating the stronger binding affinity between PV and **52–2Cu^{2+}**. Subsequent additions of a range of anions (PPI, HPO_4^{2-}, AcO^-, SO_4^{2-}, CO_3^{2-}, F^-, Cl^-, Br^- and I^-) to both **51-2Cu^{2+}-PV** and **52-2Cu^{2+}-PV** chemosensing ensembles showed that only PPi induced a significant change in the absorption spectra of either complex, with only minimal changes observed upon addition of other anions. Although both chemosensing ensembles displayed high selectivity for PPi amongst the anions tested, complex **52-2Cu^{2+}-PV**, bearing ammonium arms exhibited an approximately 527-fold greater enhancement in binding affinity to PPi than the analogue lacking the ammonium moieties. The authors attributed this significant enhancement to the cooperativity between the neighbouring ammonium groups and copper ions, which

allowed binding to PPi through a variety of interactions including electrostatic interactions, hydrogen bonding, or possibly proton transfer.

Displacement using metal ions

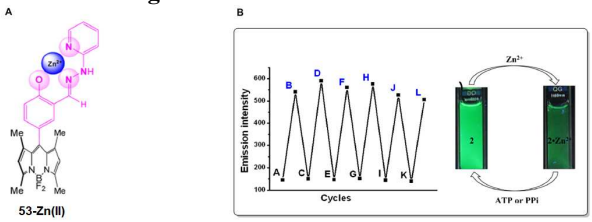

Fig. 28. A) Structure of **53-Zn^{2+}**. B) Fluorescence experiments highlighting significant and reversible "on-off" response for the detection of PPi by sensor **53-Zn^{2+}**.

Churchill and co-workers have reported a BODIPY (boron difluorodipyrromethene) based complex for the selective "turn–on" fluorescence sensing of PPi and ATP in aqueous buffer (CH_3OH:HEPES buffer, 2:1, pH 7.2) (Fig. 28A).[40] **53-Zn^{2+}** demonstrated high selectivity for ATP and PPi as indicated by a significant increase in emission intensity upon addition of these anions. The mode of sensing involves the demetallation of the weakly fluorescent **53-Zn^{2+}** by either PPi or ATP, resulting in production of the free ligand, which gives rise to the observed fluorescence enhancement. As reversibility is frequently a desired trait for sensors, this was also assessed for **53-Zn^{2+}** *via* sequential additions of PPi and Zn(II) ions. Based on the sensing mode described above, it was observed that **53–Zn^{2+}** was able to go through at least five cycles of alternating fluorescence "turn-on", "turn-off" behaviour, which renders it attractive as a reversible chemosensor. (Fig. 28B)

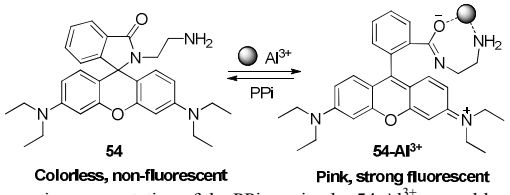

Fig. 29. Schematic representation of the PPi sensing by **54**-Al^{3+} ensemble.

A rhodamine−Al^{3+} based ensemble system was reported as a selective fluorescent and colorimetric chemosensor for PPi at pH 7.4, functioning via a metal displacement mechanism (Fig. 29).[41] The closed spirolactam ring form of **54** is colourless and non–fluorescent. On the other hand, the addition of Al^{3+} to give the spirocyclic ring–opened ensemble **54-Al^{3+}** induced a unique colour change from colourless to pink together with a large fluorescence enhancement. The addition of PPi to **54-Al^{3+}** induced fluorescence quenching and gave the original colourless solution. This was attributed to the dissociation of Al^{3+} from the complex upon addition of PPi, which clearly has a stronger affinity for Al^{3+} than **54** does, resulting in the regeneration of closed spirolactam ring as confirmed by ESI-MS experiments. This ensemble system showed a selective sensing of PPi with the addition of other biological phosphate species such as Pi, AMP, ADP and ATP resulting in no observable changes.

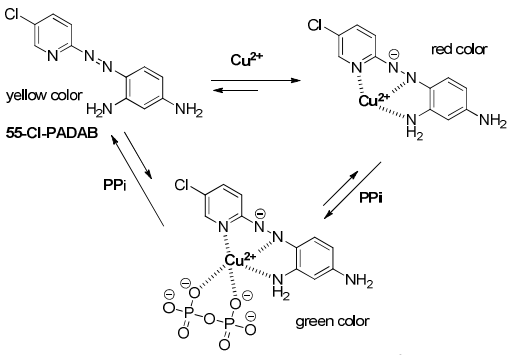

Fig. 30. Proposed binding modes of **55**−Cl−PADAB with Cu^{2+} and PPi.

Huang and co-workers utilized a Cu^{2+} complex of the commercially available 4-[(5-chloro-2-pyridyl)azo]-1,3-diaminobenzene (**55**-Cl-PADAB) as an ensemble for the selective detection of PPi (Fig. 30).[42] In an aqueous solution of hexamethylenetetramine (HMTA; 5.0×10^{-4} M) at near–neutral pH, a solution of **55**-Cl-PADAB exhibits a yellow colour with maximum absorption at 450.5 nm. The addition of Cu^{2+} induced a distinct colour change to red with a new absorption band at 506.0 nm. When 1 equiv. of PPi was added to this Cu^{2+}-**55**-Cl-PADAB complex, a new absorption band in the region of 562.0-750.0 nm appeared with a concomitant decrease of the absorption band at 506.0 nm, resulting in a colour change from red to dark green. No other anions (e.g. Pi, ATP, GTP, ppGpp) induced this type of change when added to the complex, providing a selective response to PPi, for which an association constant of 8.5×10^3 M^{-1} with 1:1 complex stoichiometry was determined. However, addition of more than 1 equiv. of PPi to Cu^{2+}-**55**-Cl-PADAB results in demetallation of the complex and the yellow colour of free 5-Cl-PADAB was observed.

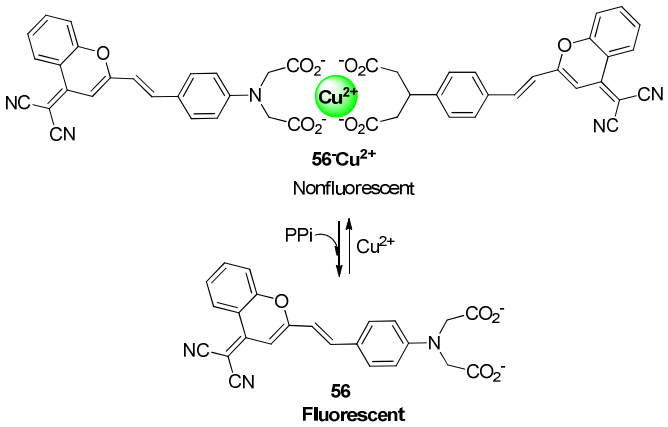

Fig. 31. Proposed mechanism of ensemble **56**-Cu^{2+} with PPi.

Zhu and co-workers reported a NIR fluorescent ensemble **56$_2$-Cu^{2+}** for PPi sensing in 100 % aqueous solution (10 mM MOPS (3-(*N*-morpholino) propanesulfonic acid), pH = 7.0) (Fig. 31).[43] Probe **56**, which bears a dicyanomethylene-4*H*-chromene as a fluorophore and an iminodiacetate group as a binding site for Cu^{2+}, exhibits NIR fluorescence at 675 nm. This fluorescence

was selectively quenched upon the addition of Cu^{2+} and an association constant for the 2:1 **56**:Cu^{2+} complex of 1.1×10^{-6} M^{-1} was determined from fluorescence titrations. The addition of PPi resulted in an enhancement of fluorescence at 675 nm, attributed to the displacement of **56** by PPi. However, full fluorescence was not restored, suggesting that the affinity of PPi towards Cu^{2+} is not strong enough to completely remove Cu^{2+} from **56_2-Cu^{2+}**. A clear colorimetric change from pale brown to red upon addition of PPi to **56_2-Cu^{2+}** was also observed by naked eye. Ensemble **56_2-Cu^{2+}** showed some selectivity for PPi over other anions although $H_2PO_4^-$, HPO_4^{2-} and PO_4^{3-} also gave small responses. The detection limit toward PPi was reported as 2.02 μM using 3 μM of **56_2**-Cu^{2+}. **56_2–Cu^{2+}** was successfully applied to the imaging of PPi in KB cells (human nasopharyngeal epidermal carcinoma cell). When cells were incubated with PPi (30 μM), turn–on fluorescence was observed in the perinuclear area of the cytosol.

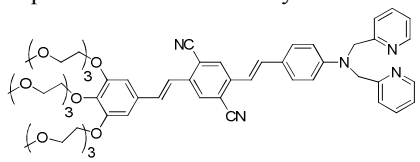

Fig. 32. Structure of two–photon probe **57**.

Qin and co-workers reported **57_2**-Cu^{2+} as a two–photon excited fluorescence probe for PPi at pH 7.4 (HEPES buffer).[44] **57** showed a broad absorption band (λ_{max} at 432 nm) due to an internal charge transfer (ICT) process (Fig. 32). Upon one photon excitation at 432 nm, the maximum wavelength of emission was 600 nm. On the other hand, two–photon fluorescence (λ_{max} = 585 nm) was examined by excitation at 740 nm. Almost complete fluorescence quenching (both one- and two-photon experiments) was observed upon addition of 0.5 equiv. of Cu^{2+} to **57**, indicating the formation of a 2:1 complex. Addition of PPi to this complex resulted in a turn-on of fluorescence, which was postulated to be a result of the displacement of one ligand from the complex. Notably, the probe **57_2**-Cu^{2+} was able to detect PPi in the presence of a large excess of PO_4^{3-} and ATP. The association constant of **57_2**-Cu^{2+} for PPi was reported to be approximately $10^{5.2}$ from the two-photon experiments, while a detection limit of 0.32 μM was determined from the one-photon experiments.

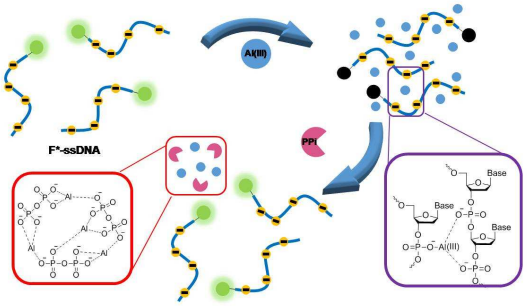

Fig. 33. Proposed binding mechanisms between F*-ssDNA and Al^{3+} and between the F*-ssDNA-Al^{3+} complex and PPi (F* stands for fluorophore).

Recently, single-stranded-DNA labelled with either FAM (Fluorescein amidite) or Cy5 fluorophores was utilized for the selective detection of PPi.[45] As shown in Fig. 33, the fluorescence of fluorophore labelled single-stranded DNA (F*-ssDNA) was quenched upon the addition of Al^{3+} at pH 7.4 (30 mM HEPES buffer). The addition of PPi led to disassociation of the F*-ssDNA-Al^{3+} complex due to the formation of the more stable Al^{3+}-PPi complex, resulting in recovery of the original fluorescence. The detection limit of this system for PPi was calculated as 40 nM with a linear range of 40 nM to 40 mM. The selectivity for PPi over Pi, ATP, AMP, ADP, dNTP and some amino acids was suggested to be a result of two factors: the stronger binding affinity of PPi for Al^{3+} due to the higher anionic charge density on the PPi oxygen atoms and increased steric hindrance for the larger nucleotide triphosphates. This system was successfully applied in the quantification of PPi in urine samples and cell lysates.

3.4. Polymer or Nanoparticle based chemosensors for PPi

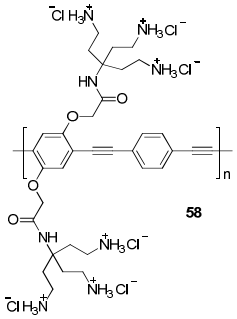

Fig. 34. Cationic poly(phenylene-ethynylene) with branched polyamine side groups (polymer **58**).

The cationic polymer, poly(phenylene-ethynylene) bearing polyamine side chains, was prepared as a selective sensor for PPi at pH 6.5 (Fig. 34).[46] Upon the addition of PPi, polymer **58** displayed a decrease in the absorption band at 400 nm with the appearance of a new band at 430 nm. Similarly, the addition of PPi induced fluorescence quenching of the original emission (433-455 nm) while a new emission band appeared at 550 nm. The red shifts in absorption as well as the blue to green emission change were attributed to conversion from the ‘‘free state’’ to the ‘‘aggregated state’’ of the polymers upon addition of PPi. The addition of PO_4^{3-}, CO_3^{2-}, SO_4^{2-}, F^-, Cl^-, Br^-, I^- or AMP did not induce any significant fluorescence change even at high anion concentrations. However, addition of ADP and ATP showed some interference for the detection of PPi using this polymer. The detection limit of **58** for PPi was calculated as 3.4×10^{-7} M.

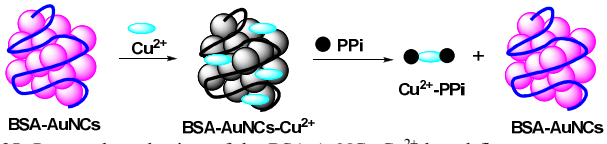

Fig. 35. Proposed mechanism of the BSA-AuNCs-Cu^{2+} based fluorescent sensor for PPi.

Bovine serum albumin (BSA) protected gold nanoclusters (AuNCs) with Cu^{2+} were reported as fluorescence sensor

systems for PPi at pH 6 (Fig. 35).[47] BSA-AuNCs displayed red fluorescence at 635 nm, which was quenched upon the addition of Cu^{2+}. This quenching was attributed to the chelation of Cu^{2+} by the glycine moieties of BSA, as characterized by high-resolution transmission electron microscopy. Addition of PPi resulted in chelation of the Cu^{2+} by the PPi, leading to dissociation of the copper ions from the BSA and a resulting 'turn-on' of fluorescence. This system shows high selectivity for PPi with a wide linear range (0.16-78.1 mM) and a detection limit of 0.083 mM.

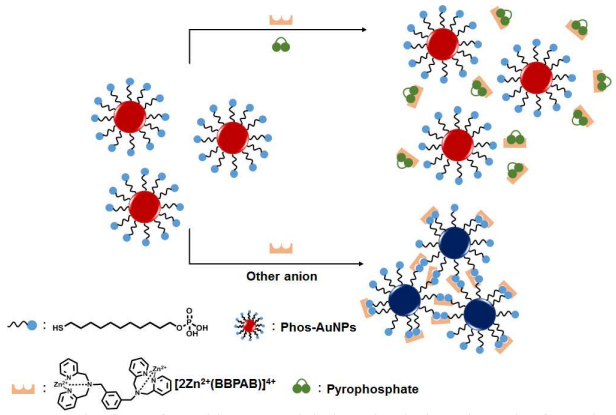

Fig. 36. Mechanism of a gold nanoparticle based colorimetric probe for PPi *via* a competition assay.

The Han group recently reported a unique system as a highly sensitive colorimetric probe for PPi, utilizing 11-mercaptoundecylphosphoric acid functionalized 13 nm gold nanoparticles (Phos-AuNPs) and [2Zn^{2+}(1,3-bis[bis(2-pyridylmethyl)aminomethyl]benzene)]$^{4+}$ ([2Zn^{2+}(BBPAB)]$^{4+}$) (Fig. 36).[48] A colour change of Phos-AuNPs from red to blue was observed upon the addition of [2Zn^{2+}(BBPAB)]$^{4+}$ as a result of [2Zn^{2+}(BBPAB)]$^{4+}$ binding to the phosphate groups and causing aggregation of the Phos-AuNPs. However, addition of a large excess of PPi was required to convert the colour of the Phos-AuNPs back to red. To avoid the requirement for addition of excess PPi, the authors pretreated [2Zn^{2+}(BBPAB)]$^{4+}$ with varying concentrations of PPi to form [2Zn^{2+}(BBPAB)(PPi)], which could bind weakly to the phosphate groups on the Phos-AuNPs (Fig. 38). The absorbance changes of the Phos-AuNPs after addition of these preincubated [2Zn^{2+}(BBPAB)(PPi)] mixtures were proportional to the decrease in PPi concentration, resulting in dramatically improved sensitivity and the PPi detection limit was reported as 146 nM. In addition, this system showed good selectivity for PPi over other common anions, AMP, ADP and ATP.

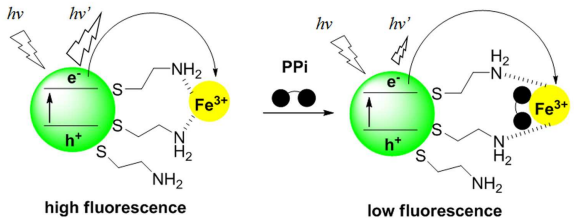

Fig. 37. Proposed mechanism of [Cys-CdS QDs]-Fe^{3+} sensing of PPi.

Fe^{3+} bound cysteamine CdS QDs ([Cys-CdS QDs]-Fe^{3+}) was recently developed as a selective fluorescence sensor for PPi at pH 7.5 (0.1 mM Tris-HCl buffer) (Fig. 37).[49] Upon the addition of PPi to [Cys-CdS QDs]-Fe^{3+}, a strong complex between Fe^{3+} and PPi is formed resulting in fluorescence quenching, which was attributed to promotion of the electron transfer process between the Fe^{3+} complex and the QDs. A linear fluorescence response for PPi was observed in the range of 0.5-10 μM with a detection limit of 0.11 μM. [Cys-CdS QDs]-Fe^{3+} displayed high selectivity for PPi over other common anions and was successfully applied to the detection of PPi in urine samples.

4. Conclusions

Selective recognition of PPi is a challenging task, requiring careful design of the sensing system. In particular, the selective detection of PPi over other phosphate species, such as Pi, ATP, ADP, AMP, etc. is difficult to achieve and the detection of PPi in biological samples requires high sensitivity and selectivity, since the PPi level in human plasma is between 1 and 5 mM while those of Pi and ATP are between 1-1.5 mM and about 1 mM, respectively.[53] Nevertheless, there have been a number of successful approaches to the selective sensing of PPi based on molecular recognition and supramolecular chemistry. Zn^{2+}-DPA derivatives on a variety of scaffolds have shown quite promising selectivity and sensitivity for PPi over Pi and ATP and successful imaging probes for PPi in cells have recently been reported. In addition, the detection of PPi in urine samples and PPi released from enzymatic reactions, including PCR, has been successfully accomplished. We believe this biologically important target will continue to draw the attention of chemists to design and develop better probes, which can selectively sense PPi with high selectivity among similar phosphate species.

Acknowledgements

J. Y. acknowledges a grant from the National Research Foundation of Korea (NRF) funded by the Korean government (MSIP) (No. 2012R1A3A2048814). K. A. J. acknowledges a grant from the Australian Research Council (DP140100227).

Notes and references

[a]Department of Chemistry and Nano Science, Ewha Womans University, Seoul 120-750, Korea. Fax: 82-2-3277-2384; Tel: 82-2-3277-2400; E-mail: jyoon@ewha.ac.kr.
[b]School of Chemistry, The University of Sydney, Sydney, NSW 2006, Australia. Fax: 61-2-9351-3329; Tel: 61-2-9351-2297; E-mail: kate.jolliffe@sydney.edu.au.
†contributed equally to this work.

1. S. K. Kim, D. H. Lee, J.-I. Hong and J. Yoon, *Acc. Chem. Res.*, 2009, **42**, 23.
2. A. E. Hargrove, S. Nieto, T. Zhang, J. L. Sessler and E. V. Anslyn, *Chem. Rev.*, 2011, **111**, 6603.
3. A. Bencini, F. Bartoli, C. Caltagirone, V. Lippolis, Dyes & Pigments, 2014, **110**, 169.
4. A. E. Timms, Y. Zhang, R. G. G. Russell, M. A. Brown, *Rheumatology*, 2002, **41**, 725.
5. S. Xu, M. He, H. Yu, X. Cai, X. Tan, B. Lu and B. Shu, *Anal. Biochem.*, 2001, **299**, 188.

6. H. T. Ngo, X. Liu and K. A. Jolliffe, *Chem. Soc. Rev.*, 2012, **41**, 4928.
7. Z. Xu, J.-Y. Choi and J. Yoon, *Bull. Kor. Chem. Soc.*, 2011, **32**, 1371.
8. C. Caltagirone, C. Bazzicalupi, F. Isaia, M. E. Light, V. Lippolis, R. Montis, S. Murgia, M. Olivari and G. Picci, *Org. Biomol. Chem.*, 2013, **11**, 2445.
9. P. Sokkalingam, D. S. Kim, H. Hwang, J. L. Sessler and C.-H. Lee, *Chem. Sci.*, 2012, **3**, 1819.
10. Z.-h. Chen, Y. Lu, Y.-b. He and X.-h. Huang, *Sens. Actuators B: Chemical*, 2010, **149**, 407.
11. Z. Zeng, A. A. Torriero, A. M. Bond and L. Spiccia, *Chem. -Eur. J.*, 2010, **16**, 9154.
12. C. Park and J.-I. Hong, *Tetrahedron Lett.*, 2010, **51**, 1960.
13. N. Shao, H. Wang, X. Gao, R. Yang and W. Chan, *Anal. Chem.*, 2010, **82**, 4628.
14. K. M. Kim, D. J. Oh and K. H. Ahn, *Chem. Asian. J.*, 2011, **6**, 122.
15. A. J. Surman, C. S. Bonnet, M. P. Lowe, G. D. Kenny, J. D. Bell, E. Tóth and R. Vilar, *Chem. -Eur. J.*, 2011, **17**, 223.
16. J. H. Lee, A. R. Jeong, J. H. Jung, C. M. Park and J.-I. Hong, *J. Org. Chem.*, 2011, **76**, 417.
17. W.-H. Chen, Y. Xing and Y. Pang, *Org. Lett.*, 2011, **13**, 1362.
18. H. J. Kim, J. H. Lee and J.-I. Hong, *Tetrahedron Lett.*, 2011, **52**, 4944.
19. B. Roy, A. S. Rao and K. H. Ahn, *Org. Biomol. Chem.*, 2011, **9**, 7774.
20. P. Das, S. Bhattacharya, S. Mishra and A. Das, *Chem. Commun.*, 2011, 47, 8118.
21. S. J. Butler and K. A. Jolliffe, *Org. Biomol. Chem.*, 2011, **9**, 3471.
22. S. J. Butler and K. A. Jolliffe, *Chem. Asian. J*, 2012, **7**, 2621.
23. X. Liu, H. T. Ngo, S. J. Butler and K. A. Jolliffe, *Chem. Sci.*, 2013, **4**, 1680.
24. J. F. Zhang, S. Kim, J. H. Han, S.-J. Lee, T. Pradhan, Q. Y. Cao, S. J. Lee, C. Kang and J. S. Kim, *Org. Lett.*, 2011, **13**, 5294.
25. D. J. Liu, G. M. Credo, X. Su, K. Wu, H. C. Lim, O. H. Elibol, R. Bashir and M. Varma, *Chem. Commun.*, 2011, **47**, 8310.
26. D.-N. Lee, A. Jo, S. B. Park and J.-I. Hong, *Tetrahedron Lett.*, 2012, **53**, 5528.`
27. S. Yang, G. Feng and N. H. Williams, *Org. Biomol. Chem.*, 2012, **10**, 5606.
28. A. S. Rao, S. Singha, W. Choi and K. H. Ahn, *Org. Biomol. Chem.*, 2012, **10**, 8410.
29. F. Huang, C. Cheng and G. Feng, *J. Org. Chem.*, 2012, **77**, 11405.
30. K. K. Yuen and K. A. Jolliffe, *Chem. Commun.*, 2013, **49**, 4824.
31. S. Anbu, S. Kamalraj, C. Jayabaskaran and P. S. Mukherjee, *Inorg. Chem.*, 2013, **52**, 8294.
32. Y. Mikata, A. Ugai, R. Ohnishi and H. Konno, *Inorg. Chem.*, 2013, **52**, 10223.
33. S. Bhowmik, B. N. Ghosh, V. Marjomaki and K. Rissanen, *J. Am. Chem. Soc.*, 2014, **136**, 5543.
34. L. G. Pathberiya, N. Barlow, T. Nguyen, B. Graham and K. L. Tuck, *Tetrahedron*, 2012, **68**, 9435.
35. Z. Guo, W. Zhu and H. Tian, *Macromolecules*, 2010, **43**, 739.
36. J. Gao, T. Riis-Johannessen, R. Scopelliti, X. Qian and K. Severin, *Dalton Trans.*, 2010, **39**, 7114.
37. R. Villamil-Ramos and A. K. Yatsimirsky, *Chem. Commun.*, 2011, **47**, 2694.
38. R. Villamil-Ramos, V. Barba and A. K. Yatsimirsky, *Analyst*, 2012, **137**, 5229
39. W. Yu, J. Qiang, J. Yin, S. Kambam, F. Wang, Y. Wang and X. Chen, *Org. Lett.*, 2014, **16**, 2220.
40. O. G. Tsay, S. T. Manjare, H. Kim, K. M. Lee, Y. S. Lee and D. G. Churchill, *Inorg. Chem.*, 2013, **52**, 10052.
41. C. R. Lohani, J. M. Kim, S. Y. Chung, J. Yoon and K. H. Lee, *Analyst*, 2010, **135**, 2079.
42. X. J. Zhao, L. He and C. Z. Huang, *Talanta*, 2012, **101**, 59.
43. W. Zhu, X. Huang, Z. Guo, X. Wu, H. Yu and H. Tian, *Chem. Commun.*, 2012, **48**, 1784.
44. Y. Li, X. Dong, C. Zhong, Z. Liu and J. Qin, *Sens. Actuators B: Chemical*, 2013, **183**, 124.
45. X. Su, C. Zhang, X. Xiao, A. Xu, Z. Xu and M. Zhao, *Chem. Commun.*, 2013, **49**, 798.
46. X. Zhao and K. S. Schanze, *Chem. Commun.*, 2010, **46**, 6075.
47. J.-M. Liu, M.-L. Cui, S.-L. Jiang, X.-X. Wang, L.-P. Lin, L. Jiao, L.-H. Zhang and Z.-Y. Zheng, *Anal. Methods*, 2013, **5**, 3942.
48. S. Kim, M. S. Eom, S. K. Kim, S. H. Seo and M. S. Han, *Chem. Commun.*, 2013, **49**, 152-154.
49. T. Noipa, K. Ngamdee, T. Tuntulani and W. Ngeontae, *Spectrochim. Acta Part A: Mol. Biomol. Spectrosc.*, 2014, **118**, 17.
50. M. W. Gorman, E. O. Feigl and C. W. Buffington, *Clin. Chem.*, 2007, **53**, 318.

Fluorescent and Colorimetric Chemosensors for Pyrophosphate

Songyi Lee, Karen K. Y. Yuen, Katrina A. Jolliffe* and Juyoung Yoon*

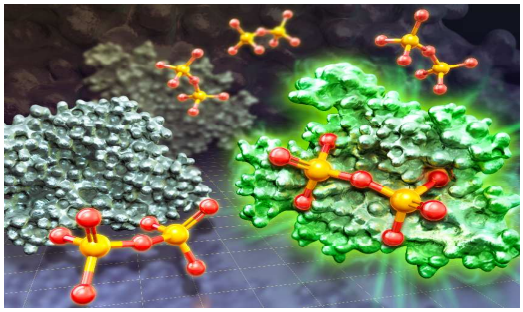

In this review, we will cover the fluorescent and colorimetric chemosensors developed for the detection of pyrophosphate (PPi) since 2010.